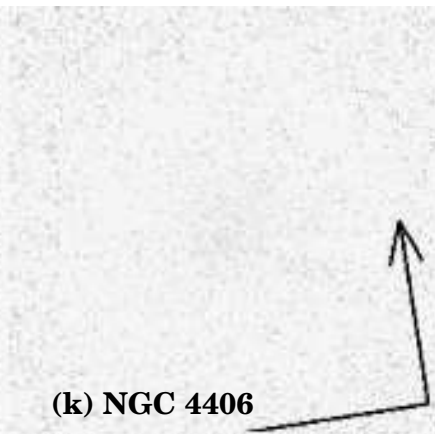
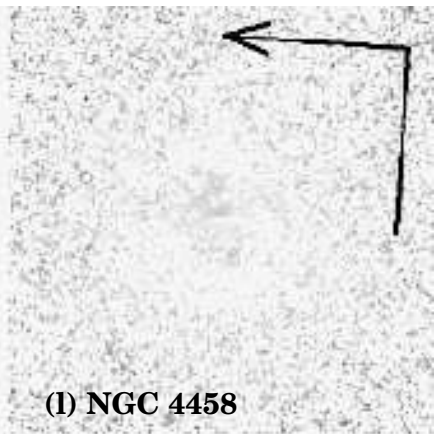


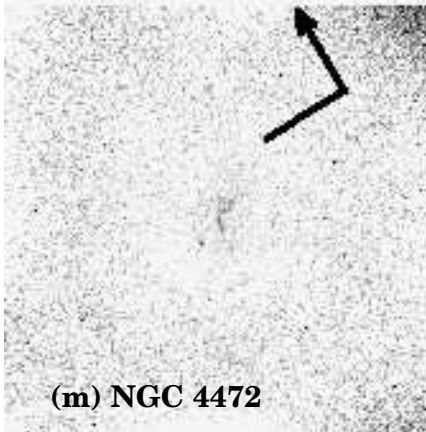
(j) NGC 4365



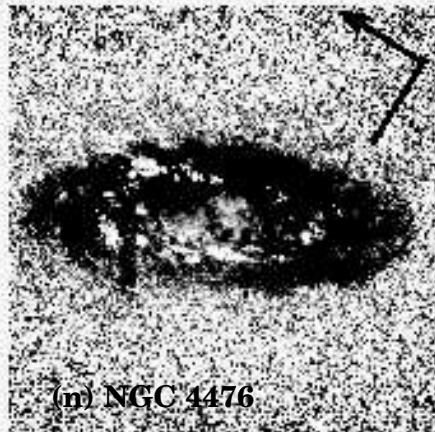
(k) NGC 4406



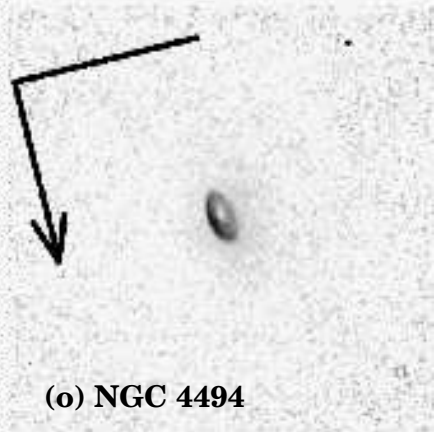
(l) NGC 4458



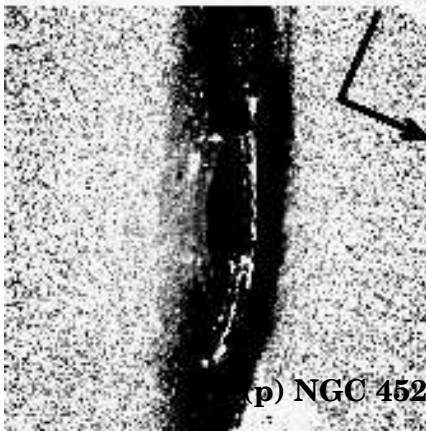
(m) NGC 4472



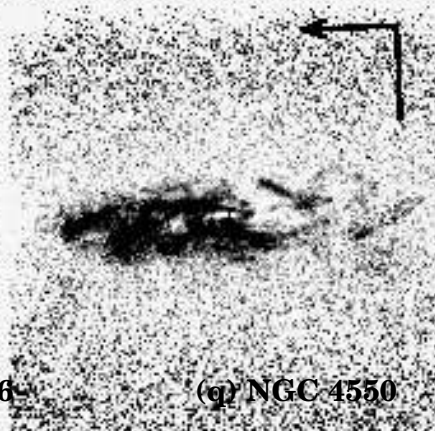
(n) NGC 4476



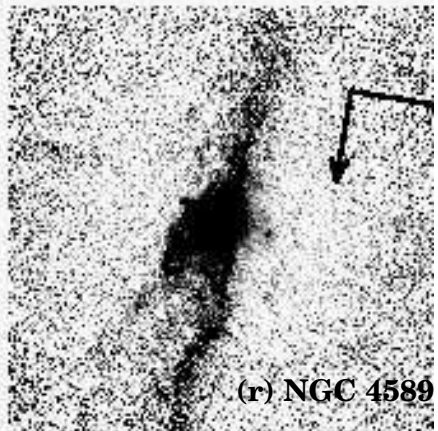
(o) NGC 4494



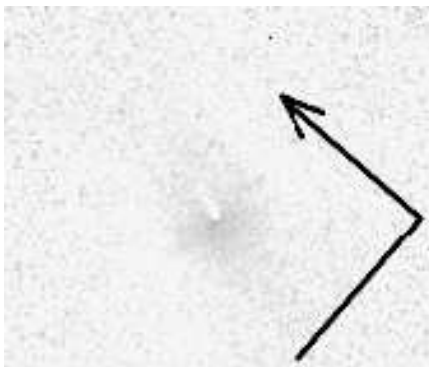
(p) NGC 4526



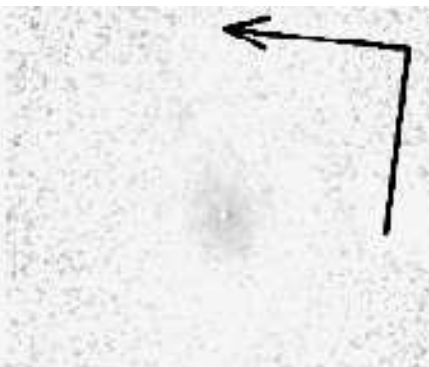
(q) NGC 4550



(r) NGC 4589



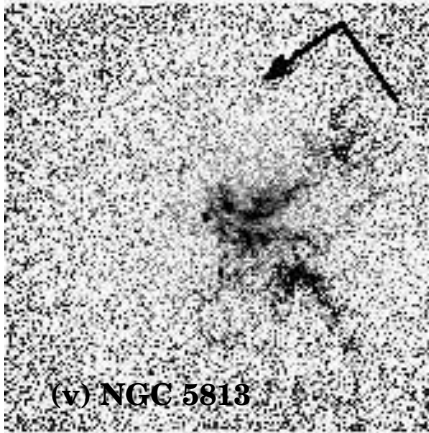
(s) NGC 4621



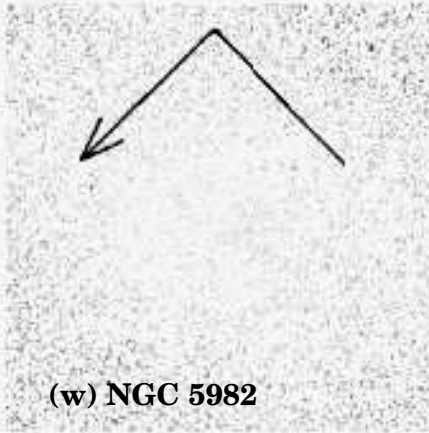
(t) NGC 4660



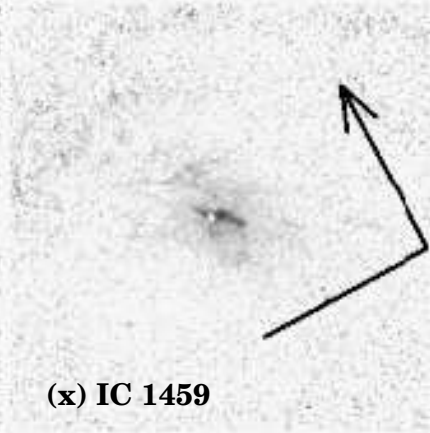
(u) NGC 5322



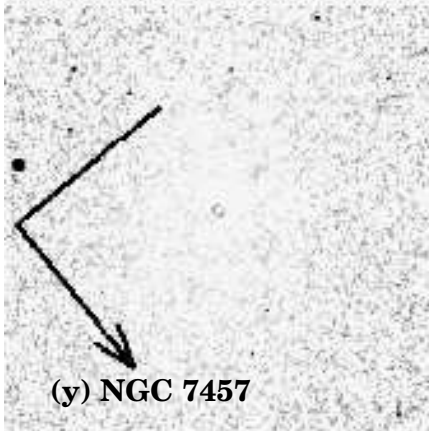
(v) NGC 5813



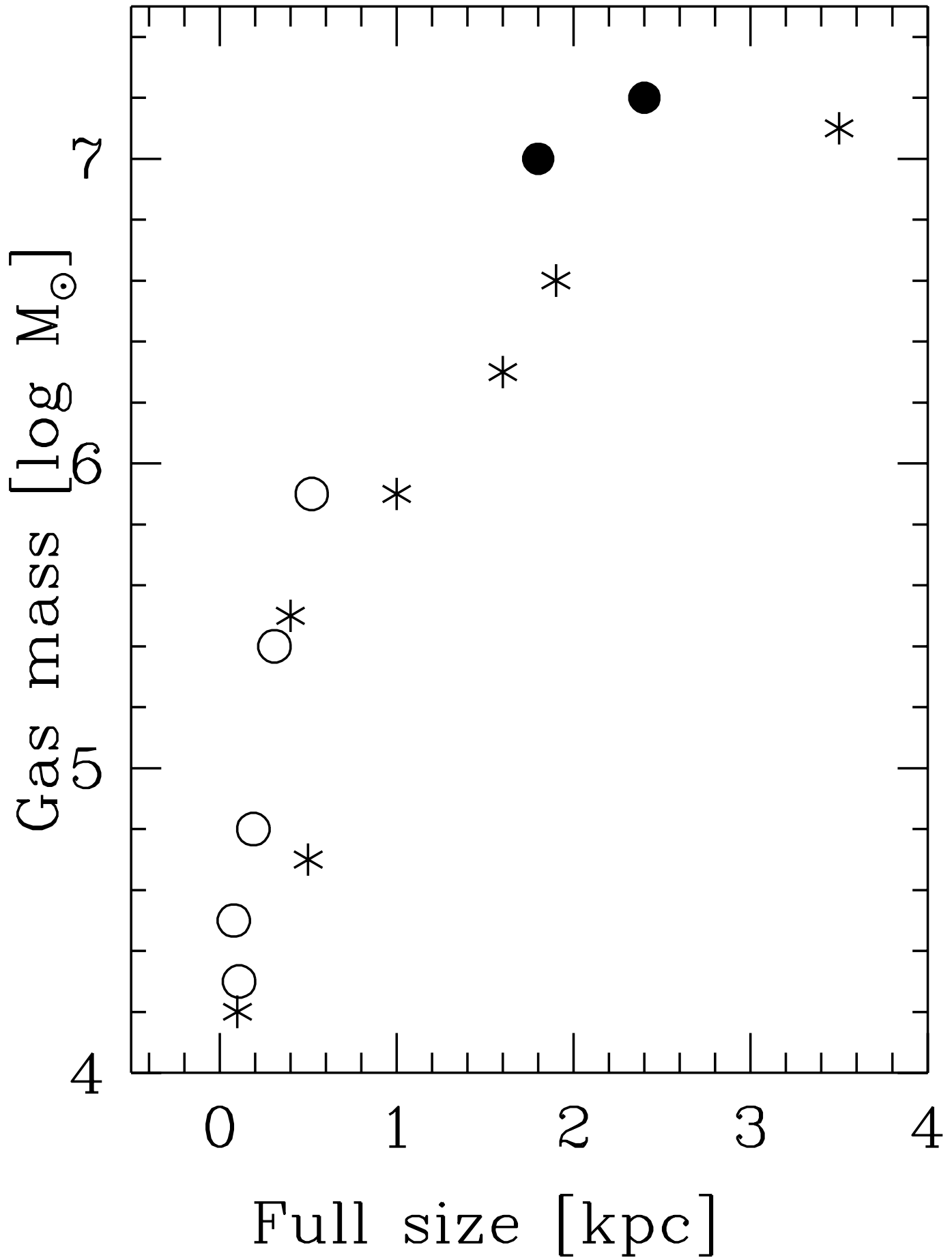
(w) NGC 5982



(x) IC 1459



(y) NGC 7457



To be appeared in AJ Vol.120, No.1 (July 2000)

## The Central Gas Systems of Early-Type Galaxies Traced by Dust Feature: Based on the HST WFPC2 Archival Images <sup>1</sup>

Akihiko Tomita<sup>2</sup>, Kentaro Aoki<sup>3,5</sup>, Masaru Watanabe<sup>3,5,6</sup>, Tadafumi Takata<sup>4</sup>, and  
Shin-ichi Ichikawa<sup>3</sup>

<sup>2</sup> Faculty of Education, Wakayama University, Wakayama 640-8510, Japan;  
atomita@center.wakayama-u.ac.jp

<sup>3</sup> National Astronomical Observatory of Japan, Mitaka, Tokyo 181-8588, Japan;  
aokikn@cc.nao.ac.jp, watanabe@aquarius.plain.isas.ac.jp, ichikawa@azuma.mtk.nao.ac.jp

<sup>4</sup> Subaru Telescope, National Astronomical Observatory of Japan, Hilo, HI 96720;  
takata@naoj.org

### ABSTRACT

We investigated the central gas systems of E/S0 galaxies by making use of the WFPC2 images of the Hubble Space Telescope archive. We searched the gas systems that were traced by the dust with a new method of making color excess images in  $F555W - F814W$  ( $V - I$ ). Out of 25 sample galaxies, we detected gas system in 14 galaxies. The dust was newly detected in two galaxies that were thought to contain no dust based on single band, pre-refurbishment data. The full extents of the gas systems are 0.1 to 3.5 kpc, and the masses of the gas,  $\log M_{\text{gas}} [M_{\odot}]$ , are 4.2 to 7.2. The AGN activity is well correlated with existence of the gas systems. None of galaxies without the gas systems show the AGN activity. On the other hand, some galaxies with the gas systems show the AGN activity; optical AGN activities are shown in 5 out of 11 galaxies of which AGNs are optically studied, and radio activities are shown in 6 out of 14 galaxies. This shows that the AGN activity is driven with the gas system.

*Subject headings:* galaxies: early-type — galaxies: gas — galaxies: dust — galaxies: active galactic nuclei — data analysis

---

<sup>1</sup> Based on observations made with the NASA/ESA Hubble Space Telescope, obtained from the data archive at the Space Telescope Science Institute, which is operated by the Association of Universities for Research in Astronomy, Inc., under NASA contract NAS 5-26555.

<sup>5</sup>Present affiliation: Japan Science and Technology Corporation, Tokyo 102-0081, Japan.

<sup>6</sup>Present address: Institute of Space and Astronautical Science, Sagami-hara, Kanagawa 229-8510, Japan.

## 1. Introduction

Early-type galaxies, E/S0 galaxies, are in general gas poor. However, some of them contain significant gas and dust in their central regions; it may be related to AGN activity, which make it be an interesting object. Jaffe et al. (1993, 1996) presented an example; they showed an HST image of central dust ring in NGC 4261, and they discussed the dust ring in connection with AGN activity. Similar dust ring structures were found in NGC 1439 and NGC 4494 by Forbes et al. (1995) and Carollo et al. (1997), and in NGC 7052 by van der Marel and van den Bosch (1998).

van Dokkum and Franx (1995) studied statistically the central gas system which were traced by the dust in early-type galaxies using the HST archives. However, they used data obtained by pre-COSTAR WF/PC camera with PC mode, and they used only one band data of  $F555W$  ( $V$  band) and without color data. Therefore, their estimates are limited by a spherical aberration of pre-refurbishment of the HST, and a detailed morphology may be missed. Though they pointed out a correlation between the gas systems and the AGN activity using radio data, we thought further discussions with post-COSTAR HST images are necessary. Though Carollo et al. (1997) studied extensively central regions of elliptical galaxies with  $F555W - F814W$  color images by WFPC2, they did not discuss the relation of gas systems with AGN phenomena in detail. Recently, Verdoes Kleijn et al. (1999) investigated the central dust in early-type galaxies based on new HST observations with multibands for a radio-loud sample. We made use of WFPC2 archival images with two bands,  $F555W$  ( $V$  band) and  $F814W$  ( $I$  band), and investigated the central gas system traced by dust more precisely by making and analyzing color excess images for early-type galaxies with or without AGN activities. In section 2 we describe sample and a new method of data analysis. We give results in section 3; how frequent the gas systems are observed, and how much are those masses, and what are those morphologies. We discuss the characteristics of the gas system in connection with AGN activity in section 4. Conclusions are given in section 5.

## 2. Data and Reduction

### 2.1. The data

Among a large number of galaxies in the HST archive, we restricted sample to galaxies that satisfy following criteria: (1) objects were taken with WFPC2. (2) objects were taken with both  $F555W$  ( $V$  band) and  $F814W$  ( $I$  band) filters; color excess image is necessary to investigate the gas system in detail, and a combination of  $F555W$  and  $F814W$  gave the largest in data frame number. (3) position of galactic center was taken on the PC chip; PC chip has a better spatial resolution than WF chips. A pixel size of the PC chip was  $0''.0455$ . (4) objects are elliptical (E) or lenticular (S0) in morphology; morphological type was obtained by NED (NASA Extragalactic Database). (5) objects reside at suitable distance; objects in the Local Group were excluded because of too much proximity compared with other objects, and objects with heliocentric radial

velocity of  $v_{\text{helio}} > 3000 \text{ km s}^{-1}$  were excluded. The radial velocity was obtained by NED. (6) objects with NGC or IC numbers; we reduced number of sample in order to analyze the data in detail intending to avoid a bias to active galaxies or peculiar galaxies.

In August 1996 we searched the HST archive and found 25 galaxies which satisfy the criteria above. The image data we requested and received were bias and dark subtracted, and flat-fielded ones. Typical exposure time of one frame was a few times 100 s. The sample is listed in table 1; we referred to Nearby Galaxies Catalog by Tully (1988) for reliable distance to galaxy and tabulated in the fifth column. We should note that 12 of total 25 were observed under a program of ‘ellipticals with kinematically distinct cores’ and published by Carollo et al. (1997); these objects are shown by asterisks in the last column of table 1. There is a bias for kinematically distinct cores in our sample.

## 2.2. Making color image

In processing the images, we used IRAF <sup>7</sup> and STSDAS <sup>8</sup>. We at first removed cosmic ray events on the CCD chip by using an STSDAS task of *crrej* with two to several sequential frames which had the same pointing and pass bands. By combining the processed frames, we obtained a set of two images, through *F555W* and *F814W* filters, for each of 25 sample galaxies with a high signal-to-noise ratio.

The extinction or color excess is due to dust in the gas system, and we recognize the gas system by seeing the pattern of the extinction or color excess on image. Since gradient of intensity profile is very steep in the central region of galaxy, it is difficult to estimate the extinction. On the other hand, the color gradient is much flat even in the central region of galaxy, therefore, we obtained values of the color excess more reliably. Thus, we made and analyzed color excess images rather than intensity images only. This is a new method for analyzing the gas systems.

The color image of *F555W* – *F814W*, hereafter we write it simply as  $V - I$ , is derived by processing as

$$V - I = -2.5 \log_{10} i(V)/i(I),$$

where  $i(V)$  and  $i(I)$  are intensities, namely CCD counts, in *F555W* and *F814W*, respectively. The bands of  $V$  and  $I$  denoted here are in the ST system and they closely correspond to the Johnson  $V$  and Cousins  $I$  bands, respectively. A detailed description is given in the WFPC2 Instrument Handbook (Biretta et al. 1996). We carefully checked the position matching between images with

---

<sup>7</sup>IRAF is the software developed in National Optical Astronomy Observatories.

<sup>8</sup>STSDAS is the software developed in Space Telescope Science Institute.

two bands. We found artificial symmetric patterns in  $V - I$  images of NGC 1427, 3610, and 4660 which seem to be caused by shear in position. We shifted images by every 0.1 pixel and found the matched position, and obtained correct  $V - I$  image.

### 2.3. Inspection for the gas system

By careful inspection of the  $V - I$  images, we found features caused by dust in 14 galaxies. The color excess image in  $V - I$  was made as

$$E(V - I) = (V - I) - (V - I)_{\text{intrinsic}} = -2.5 \log ( [i(V)/i(I)] / [i(V)/i(I)]_{\text{intrinsic}} ),$$

where  $(V - I)_{\text{intrinsic}}$  means  $V - I$  color without reddening due to dust.  $[i(V)/i(I)]_{\text{intrinsic}}$  was estimated by fitting the  $V - I$  image masking the regions where we found features by dust. We inspected the  $E(V - I)$  images if there were other features by dust which had not been found in inspecting the  $V - I$  image. When we found new features, we again made the fitting. Note that with circular or ring-like mask, the elliptical isophote fitting task of *ellipse* in STSDAS does not fit the masked region. The fitting was made by an IRAF task of *imsurfit*. We fitted to  $1 \times 1$  order and  $2 \times 2$  order curved surfaces of spline with degree 1, spline with degree of 3, and legendre functions, and took one which was the most successful for the fitting. Thus, we obtained  $E(V - I)$  image for each of 25 sample galaxies.

The derived  $E(V - I)$  images are shown in figure 1; gray scale is expressed in magnitude scale, and white level indicates  $E(V - I) \leq 0.0$  mag, and black level indicates  $E(V - I) \geq 0.2$  mag. Size and mass of the gas system traced by the dust were inspected in these  $E(V - I)$  images. The background noise of the  $E(V - I)$  image is about 0.03 mag. We plotted contour map with a binning of  $3 \times 3$  pixels, which made the contour of 0.03 mag to be three times of noise level in the plotted figure. We recognized the dust regions by finding places over the threshold of 0.03 mag in the contour map with the binning. If we found no significant patterns above this threshold, we describe it as non-detection. We should note that we have difficulty in detection of the dust region in the case that way of dust distribution is the same as that of color or intensity profile, or like a thin face-on disk.

### 2.4. Deriving mass of the gas system

We measured mass of the gas system through area-integrated  $E(V - I)$  and a Galactic conversion factor. The integrated  $E(V - I)$  was measured by summation of count in  $E(V - I)$  image within areas that include the dust regions we detected. The conversion factor is obtained as follows.

van Dokkum and Franx (1995) used a relation between  $A_V$  and dust mass and they took Galactic value for coefficient. Taking gas-to-dust ratio of 100, this gives

$$M_{\text{gas}} / E(B - V) = 1.4 \times 10^{-2} \text{ [ g cm}^{-2} \text{ mag}^{-1}\text{]};$$

assuming that mass ratio of hydrogen and helium is 0.75 to 0.25, a relation of hydrogen gas column density ( $N_{\text{H I}}$ ) and  $E(B - V)$  (e.g., Diplax and Savage 1994) gives the same result. Taking Galactic value of  $E(V - I) / E(B - V) = 1.6$  by Rieke and Lebofsky (1985), we obtained

$$M_{\text{gas}} \text{ (per CCD pixel on the PC chip)} / E(V - I) = 2.0 \times D^2 \text{ [ } M_{\odot} \text{ pix}^{-1} \text{ mag}^{-1}\text{]},$$

where  $D$  is distance to galaxy in the unit of Mpc. The above derivation is based on the screen model that dust shield lies in front of light source in the line of sight. As a matter of fact, the gas system lies inside the galaxy. We doubled the color excess in calculating mass of the gas system; an error of a factor of a few times ten percent is considered to be introduced through this procedure. Thus, we used an equation

$$M_{\text{gas}} \text{ [} M_{\odot} \text{]} = 4.0 \times D^2 \int_{\text{area}} E(V - I) d(\text{pixel}).$$

Including the errors introduced by using Galactic value and in summation of  $E(V - I)$ , total error in logarithmic scale in above equation is considered to be about 0.3 to 0.5 depending on signal-to-noise ratio and size of the region.

### 3. Results

#### 3.1. Frequency of the gas system

In table 2, we summarize the detection of the gas system traced by dust. The gas systems were detected in 14 out of 25 sample galaxies; more than a half, 56%, of early-type galaxies shows the gas system in the central region. This result is consistent with result by van Dokkum and Franx (1995) that the gas systems were detected in 48% of their sample galaxies. Among our sample, all of the gas systems which were detected by van Dokkum and Franx (1995) were found by us. Among their sample, we newly detected the dust feature in NGC 3377 and NGC 3608 which has not been detected. This is because we used images taken after the 1993 refurbishment mission and a new method of inspecting color excess images. Though we saw a possible dust feature in NGC 4458, the criterion described in subsection 2.3 was not satisfied in this case. We checked a distance bias in the detection rate. We detected the dust features in 4 out of 6 galaxies with  $D \leq 10$  Mpc, 6 out of 13 galaxies with  $10 < D \leq 20$  Mpc, and 4 out of 6 galaxies with

$D > 20$  Mpc. Though the number of sample is small and the statistics are poor, the frequency does not show a dependence on distance.

For galaxies with the kinematically distinct cores, the detection rate of the gas system is 8 out of 12, and for other galaxies, 6 out of 13. Though the number of sample is small and the statistics are poor, it seems that the detection rate for galaxies with the kinematically distinct cores is a little higher than or the same as that for others. Verdoes Kleijn et al. (1999) detected the dust features in 17 out of 19 radio-loud E/S0 galaxies. A high detection rate for galaxies with AGNs is discussed in section 4.

### 3.2. Size of the gas system

The full extent of the dust distribution,  $d$ , was measured and is listed in the fourth column of table 2. The smallest size is 0.08 kpc for NGC 4494, and the largest is 3.5 kpc for NGC 4589. The dust distribution seems to extend to out of the frame for NGC 4589, and possibly for NGC 3377 as well.

### 3.3. Mass of the gas system

Mass of the gas system traced by the dust,  $M_{\text{gas}}$ , was derived as is explained in subsection 2.4, and results are tabulated in the fifth column of table 2. The smallest mass is  $\log M_{\text{gas}} [M_{\odot}] = 4.2$  for NGC 4472 and the largest mass is 7.2 for NGC 4526. Note that for NGC 4476 and NGC 4526, there are many HII regions on the dust, thus, the derived masses seem to be underestimated and to contain larger errors. The upper limit of gas mass for objects without detection is considered to be about 3.5 in logarithmic solar mass unit.

van Dokkum and Franx (1995) reported masses of the gas systems, and most of their sample is included in our sample. Their estimation of mass is tabulated in the sixth column of table 2; these values are converted using distances given by Tully (1988) which we show in table 1. In some galaxies, our results are consistent with results by van Dokkum and Franx (1995), and in other galaxies our results are about an order of magnitude larger than those by van Dokkum and Franx (1995). For instance, we derived  $\log M_{\text{gas}} [M_{\odot}] = 5.5$  for IC 1459, while it was 4.9 by van Dokkum and Franx (1995) after the conversion considering the distance. van Dokkum and Franx (1995) described that the morphology of the gas system to be ‘warped lane’. We found extended dust distribution around the warped lane (see the first paragraph of subsection 3.4). Limiting to the lane region, our estimation was  $\log M_{\text{gas}} [M_{\odot}] = 4.7$ , which is consistent with the result by van Dokkum and Franx (1995) considering the error. Taking a new method, the mass estimation is revised.

### 3.4. Morphology of the gas system

In inspecting the dust regions as described in subsection 2.3, we obtained the contour plots with the threshold of  $E(V - I) = 0.03$  mag. Six samples, NGC 1439, 3379, 4476, 4494, 4526, and 5322, have the outer contours of  $E(V - I) = 0.03$  mag that could be fitted by an ellipse with its center on the galactic center. Others have irregular outer contours and barycenters of the dust distributions are off the galactic centers. Though the signal-to-noise ratio is poor for NGC 3608, by a careful image inspection we found the dust region in NGC 3608 to belong to the former group. We call the former group ‘disky’ and the latter group ‘irregular’ in morphology of the gas system. Though we assigned ‘irregular’ for IC 1459, it has also a ‘disky’ feature. With a contour of  $E(V - I)$  of 0.1 mag, we found a disk component (see the second paragraph in subsection 3.3). Verdoes Kleijn et al. (1999) also made a classification of the dust features. Our disk category corresponds to their classes of disks and lanes. We should note their argue that difference between disks and lanes is not solely due to different viewing angles.

In figure 2, we plot the size and mass distributions of the gas systems. The signs of plots indicate morphologies of the gas systems; a circle denotes the disk type and an asterisk denotes the irregular type. For the irregular group, the size and mass frequency are flat;  $\log M_{\text{gas}} [M_{\odot}]$  is from 4.2 to 7.1, and  $d$  is from 0.1 to 3.5 kpc. On the other hand, for the disk group, they are bimodal; 5 out of 7 samples have  $\log M_{\text{gas}} [M_{\odot}]$  of  $5.0 \pm 0.6$  and  $d$  of  $0.24 \pm 0.16$  kpc, while other two samples, NGC 4476 and NGC 4526, have  $\log M_{\text{gas}} [M_{\odot}]$  of  $7.1 \pm 0.1$  and  $d$  of  $2.1 \pm 0.3$  kpc. We call the former ‘small disk’ and the latter ‘large disk’. In figure 2, we plot the small disks with open circles, and the large disks with filled circles. The large disks are only samples which have the H II regions. Considering also that morphologies of the host galaxies with the large disks are S0’s, the large disks seem to be normal gas disks which are commonly seen in spiral galaxies. The central gas ring in NGC 4261 presented by Jaffe et al. (1993, 1996) would belong to the small disk group; this object is not included in our sample. Radii of disks in our small disk group sample are from 40 to 260 pc, which are comparable to the radius of the ring in NGC 4261 of 140 pc; we converted a result by Jaffe et al. (1993) using a distance of 35.1 Mpc given in Tully (1988) instead of 14.7 Mpc which was used in Jaffe et al. (1993).

### 3.5. Blue nuclei and nuclear disks

In some  $E(V - I)$  images, we found point-like nuclei. Carollo et al. (1997) and Verdoes Kleijn et al. (1999) also reported these objects. These are found in NGC 4278, 4365, 4458, 4476, 4660, and 7457, and IC 1459. The nucleus has a slightly bluer color than surrounding area, and the color excesses are of order of 0.1 mag for NGC 4278, 4476, and 7457, and IC 1459, and of order of 0.01 mag for others. In NGC 3115, 3377, 3384, 3610, and 4621, CCD counts near the nuclei are saturated, thus, it is not clear whether these have the blue nuclei. Since the blue nucleus has a cuspy intensity peak, most of the saturated nuclei may have the blue nuclei.

By inspecting the  $V$ -band images, we found structures like nuclear disks with size of 100 pc scale in NGC 3115, 4550, and 4621. The disk-like structure has a slightly bluer color than surrounding area, and the color excesses are of order of 0.1 mag for NGC 4550, and of order of 0.01 mag for others. Therefore, we recognized the structures also in  $E(V - I)$  images. The structure in NGC 3115 was previously reported by Kormendy et al. (1996).

#### 4. Discussion

van Dokkum and Franx (1995) showed that the gas systems came from outside the galaxies by presenting a misalignment of position angles for the gas system and the host galaxy. We discuss here the connection of the infalling gas systems with the AGN activity.

Ho et al. (1997) investigated optical AGN properties of nearby galaxies. The AGN properties for our sample galaxies are listed in the seventh column of table 2. We grouped result by Ho et al. (1997) into three: AGN group which contains objects with L1.9, L2 (L for LINER), S2 (S for Seyfert), and T2 (T for Transition between LINER and H II nucleus), and includes objects with the sign of ‘:’, non-AGN group which contains objects with NO and H (H for H II nucleus), and objects with the sign of ‘::’ because of very weak emission lines, and ‘no data’ group which contains objects without observations by Ho et al. (1997), which is signed as ‘—’ in table 2. Among 25 sample galaxies, 20 galaxies were observed by Ho et al. (1997). The optical AGN activities are found in 1 out of 6 galaxies with  $D \leq 10$  Mpc, 1 out of 8 galaxies with  $10 < D \leq 20$  Mpc, and 3 out of 6 galaxies with  $D > 20$  Mpc. There is an indication of little distance bias in the AGN detection that it is easier to detect the AGN activities in nearer galaxies. The existence of the AGN activity is correlated with existence of the gas systems. None of 9 galaxies without detection of the gas systems are grouped in AGN group, and 5 out of 11 galaxies with gas systems shows AGN activity. This indicates that the gas system which can be found in the HST WFPC2 archival image is necessary for the present AGN activity.

Radio emission is considered to be related to the AGN. The 4.85 MHz survey in the northern hemisphere was made by Gregory and Condon (1991) using Green Bank 91m radio telescope and compiled as 87GB catalog; among our sample, 24 galaxies except IC 1459 are included in this survey region. NGC 4278, 4472, 4589, and 5322 were detected in this survey. 4.85 MHz survey in the southern hemisphere was made using Parkes 64m radio telescope and compiled as Parkes-MIT-NRAO (PMN) catalog; IC 1459 was detected and described in Wright et al. (1996). According to NED, NGC 5813 is another radio source detected by White and Becker (1992), though it is not cataloged in 87GB catalog. We took above six galaxies as radio galaxies and indicated in the eighth column of table 2. The radio activities are found in 1 out of 6 galaxies with  $D \leq 10$  Mpc, 2 out of 13 galaxies with  $10 < D \leq 20$  Mpc, and 3 out of 6 galaxies with  $D > 20$  Mpc. There is an indication of little distance bias in the radio detection that it is easier to detect the radio in nearer galaxies. Though being a radio galaxy is not so tightly correlated with the optical AGN properties by Ho et al. (1997), correlation of the existence of the gas system

with being a radio galaxy is similar to that with the optical AGN properties. None of 11 galaxies without the gas systems are radio galaxies and 6 out of 14 galaxies with gas systems is radio galaxy. van Dokkum and Franx (1995) gave similar results. Verdoes Kleijn et al. (1999) made observations of 19 nearby radio-loud early-type galaxies using the HST WFPC2, and reported that they detected the dust in all but two galaxies. This supports the high detection rate of the gas system in galaxies with the AGN.

The gas mass seems to be independent of the AGN existence. In the optical activity, those with the AGN have  $\log M_{\text{gas}} [M_{\odot}] = 4.8$  to 7.1 and those without the AGN have 4.2 to 7.2; in the radio activity, the radio galaxies have 4.2 to 7.1 and others have 4.3 to 7.2. Morphology of the gas system shows rather clear contrast in the AGN existence, though the statistics are poor. In the optical activity, within the Ho et al. (1997) sample, one of four disk-like gas systems, and four of six irregular gas systems have the AGNs; in the radio activity, one of seven disk-like gas systems, and five of seven irregular gas systems are radio galaxies. The gas system with an irregular morphology may be infalling more effectively than that with a disk-like morphology. This suggests that efficiency in infalling of the gas to the nucleus is correlated in driving the AGN activity.

The blue nucleus may be AGN or young star cluster originated from the gas system. However, existence of the blue nucleus is not correlated with existence of AGN, and not correlated with existence or morphology of the gas system either; its nature is unclear. Since NGC 4550 possesses a type-II LINER, the nuclear disk-like structure in NGC 4550 may be strong light beams escaping from nucleus to the direction which is perpendicular to line of sight considering the blueness of the structure. However, the same cases are not seen in other type-II LINERs.

## 5. Conclusions

We investigated the gas systems in the central regions of 25 E/S0 galaxies by analyzing the color excess images made from HST archives. The conclusions are:

1. We detect the central gas systems that can be traced by the dust in 14 out of 25 sample galaxies. We find the gas system in two galaxies that were reported to be dust-free by van Dokkum and Franx (1995) which was based on single band, pre-refurbishment data.
2. The morphologies of the gas systems are grouped into three: small disk, large disk, and irregular system. For small disk, full extent of  $d$  is 0.1 to 0.5 kpc and gas mass of  $\log M_{\text{gas}} [M_{\odot}]$  is 4.3 to 5.9. For large disk,  $d$  is about 2 kpc and  $\log M_{\text{gas}} [M_{\odot}]$  is about 7. For irregular system,  $d$  is 0.1 to 3.5 kpc and  $\log M_{\text{gas}} [M_{\odot}]$  is 4.2 to 7.1.
3. The AGN activity is well correlated with existence of the gas system which can be found in the HST WFPC2 archival image.
4. The AGN activity is triggered by an infalling gas system with a probability of about 50%, and the probability is higher if the morphology of the gas system is seen as irregular type, though the

statistics are poor.

We thank an anonymous referee for careful reading and making valuable comments, which improved this paper very much. This research was financially supported by joint research of National Astronomical Observatory of Japan in 1997 and 1998. This research made use of Astronomical Data Analysis Center of National Astronomical Observatory of Japan. This research made use of the NASA/IPAC Extragalactic Database (NED) which is operated by the Jet Propulsion Laboratory, Caltech, under contact with the National Aeronautics and Space Administration.

## REFERENCES

- Biretta, J., et al. 1996, Wide Field and Planetary Camera 2 Instrument Handbook, Version 4.0 (Baltimore: STScI)
- Carollo, C. M., Franx, M., Illingworth, G. D., and Forbes, D. A. 1997, ApJ, 481, 710
- Diplas, A. and Savage, B. D. 1994, ApJ, 427, 274
- Forbes, D. A., Franx, M., and Illingworth, G. D. 1995, AJ, 109, 1988
- Gregory, P. C. and Condon, J. J. 1991, ApJS, 75, 1011
- Ho, L. C., Filippenko, A. V., and Sargent, W. L. W. 1997, ApJS, 112, 315
- Jaffe, W., Ford, H. C., Ferrarese, L., van den Bosch, F., and O’Connell, R. W. 1993, Nature, 364, 213
- Jaffe, W., Ford, H. C., Ferrarese, L., van den Bosch, F., and O’Connell, R. W. 1996, ApJ, 460, 214
- Kormendy, J., Bender, R., Richstone, D., Ajhar, E. A., Dressler, A., Faber, S. M., Gebhardt, K., Grillmair, C., Lauer, T. R., and Tremaine, S. 1996, ApJ, 459, L57
- Rieke, G. H. and Lebofsky, M. J. 1985, ApJ, 288, 618
- Tully, R. B. 1988, Nearby Galaxies Catalog (Cambridge University Press: Cambridge)
- van der Marel, R. P. and van den Bosch, F. C. 1998, AJ, 116, 2220
- van Dokkum, P. G. and Franx, M. 1995, AJ, 110, 2027
- Verdoes Kleijn, G. A., Baum, S. A., de Zeeuw, P. T., and O’Dea, C. P. 1999, AJ, 118, 2592
- White, R. L. and Becker, R. H. 1992, ApJS, 79, 331
- Wright, A. E., Griffith, M. R., Hunt, A. J., Troup, E., Burke, B. P., and Ekers, R. D. 1996, ApJS, 103, 145

Fig. 1.—  $E(V - I)$  images of 25 sample galaxies. Gray Scale is expressed in magnitude scale, and white level indicates a color excess of 0 mag or less and black level indicates a color excess of 0.2 mag or more. Field of view is central  $256 \times 256$  pixels, which gives  $11''.6 \times 11''.6$ , or central  $512 \times 512$  pixels, which gives  $23''.3 \times 23''.3$  for objects with large-sized gas systems. The direction of north and east is indicated by a sign of arrow and bar; the direction of the arrow shows the north. The length of the arrow corresponds to  $5''$ . (a) NGC 1427, (b) NGC 1439, (c) NGC 3115, (d) NGC 3377; the up-turn feature at upper edge is artificial, (e) NGC 3379, (f) NGC 3384, (g) NGC 3608, (h) NGC 3610, and (i) NGC 4278.

Fig. 1.— Continued. (j) NGC 4365, (k) NGC 4406, (l) NGC 4458, (m) NGC 4472, (n) NGC 4476, (o) NGC 4494, (p) NGC 4526, (q) NGC 4550, and (r) NGC 4589.

Fig. 1.— Continued. (s) NGC 4621, (t) NGC 4660, (u) NGC 5322, (v) NGC 5813, (w) NGC 5982, (x) IC 1459, and (y) NGC 7457.

Fig. 2.— The diagram showing size and mass distributions of fourteen gas systems detected by us. Open circle indicates the gas system with a small disk morphology, filled circle indicates that with a large disk morphology, and asterisk indicates that with irregular morphology.

Table 1. SAMPLE GALAXIES

(1) No.	(2) Name	(3) Morphology	(4) $v_{\text{helio}}$ [km s <sup>-1</sup> ]	(5) $D$ [Mpc]	(6)
1	NGC 1427	E5	1416	16.9	*
2	NGC 1439	E1	1670	19.7	*
3	NGC 3115	S0 <sup>-</sup>	663	6.7	
4	NGC 3377	E5 - 6	692	8.1	
5	NGC 3379	E1	920	8.1	
6	NGC 3384	SB(s)0 <sup>-</sup> :	735	8.1	
7	NGC 3608	E2	1108	23.4	*
8	NGC 3610	E5:	1787	29.2	
9	NGC 4278	E1 - 2	649	9.7	*
10	NGC 4365	E3	1240	16.8	*
11	NGC 4406	S0(3)/E3	-227	16.8	*
12	NGC 4458	E0 - 1	668	16.8	
13	NGC 4472	E2/S0(2)	868	16.8	
14	NGC 4476	SA(r)0 <sup>-</sup> :	1958	16.8	
15	NGC 4494	E1 - 2	1324	9.7	*
16	NGC 4526	SAB(s)0 <sup>0</sup> :	448	16.8	
17	NGC 4550	SB0 <sup>0</sup> :	381	16.8	
18	NGC 4589	E2	1980	30.0	*
19	NGC 4621	E5	424	16.8	
20	NGC 4660	E:	1097	16.8	
21	NGC 5322	E3 - 4	1915	31.6	*
22	NGC 5813	E1 - 2	1924	28.5	*
23	NGC 5982	E3	2904	38.7	*
24	IC 1459	E	1691	20.0	*
25	NGC 7457	SA(rs)0 <sup>-</sup> ?	824	12.3	

Notes:

Column (3): morphology taken from NED. Column (4): heliocentric radial velocity taken from NED. Column (5): distance taken from Tully (1988). The data for NGC 5982 is not given in Tully (1988), therefore, we give distance as  $(v_{\text{helio}} [\text{km s}^{-1}] / 75.0) [\text{Mpc}]$ . Column (6): WFPC2 observations of galaxies with asterisks were published by Carollo et al. (1997).

Table 2. RESULT OF MEASUREMENTS OF THE GAS SYSTEM

(1) No.	(2) Name	(3) Dust morphology	(4) Size [kpc]	(5) $\log M_{\text{gas}}$ [ $M_{\odot}$ ]	(6) vD&F	(7) AGN?	(8) radio?	(9) comments
1	NGC 1427	NO				—		
2	NGC 1439	small disk	0.31	5.4	3.6	—		
3	NGC 3115	NO			NO	NO		sat, disk
4	NGC 3377	irregular	0.5	4.7	NO	NO		sat
5	NGC 3379	small disk	0.11	4.3	3.5	L2/T2::		
6	NGC 3384	NO			NO	NO		sat
7	NGC 3608	small disk	0.19	4.8	NO	L2/S2:		
8	NGC 3610	NO				NO		sat
9	NGC 4278	irregular	1.0	5.9	5.3	L1.9	yes	nuc
10	NGC 4365	NO			NO	NO		nuc
11	NGC 4406	NO				NO		
12	NGC 4458	NO				—		nuc
13	NGC 4472	irregular	0.1	4.2	3.1	S2::	yes	
14	NGC 4476	large disk	1.8	7.0	6.1	—		nuc
15	NGC 4494	small disk	0.08	4.5	3.5	L2::		
16	NGC 4526	large disk	2.4	7.2		H		
17	NGC 4550	irregular	1.6	6.3	5.4	L2		disk
18	NGC 4589	irregular	3.5	7.1	5.8	L2	yes	
19	NGC 4621	NO			NO	NO		sat, disk
20	NGC 4660	NO				NO		nuc
21	NGC 5322	small disk	0.52	5.9	5.7	L2::	yes	
22	NGC 5813	irregular	1.9	6.6	4.9	L2:	yes	
23	NGC 5982	NO			NO	L2::		
24	IC 1459	irregular	0.4	5.5	4.9	—	yes	nuc
25	NGC 7457	NO			NO	NO		nuc

Notes:

Column (4): Full extent of the gas system. Column (5): Upper limit for without detection is estimated about 3.5. Column (6): Mass estimated by van Dokkum and Franx (1995) in logarithmic solar mass unit, and converted using distances given by Tully (1988). ‘NO’ means that they did not detect the gas system, and blank means it was not included in their sample. Column (7): AGN property is taken from Ho et al. (1997). NO: No emissions were detected neither around the  $H\alpha$  nor the  $H\beta$  lines. L1.9: LINER with a weak broad-line component in the  $H\alpha$  line. L2: LINER without the broad-line component. S2: Type-II Seyfert nucleus. H: H II nucleus. T2: Transition object between LINER and H II nucleus. The sign of ‘:’ means the classification is uncertain, and ‘::’ means the classification is highly uncertain. Objects that are not included in Ho et al. (1997) are denoted as ‘—’. Column(9): sat: CCD count near the nucleus is saturated. nuc: A blue point-like source is seen at the nucleus of galaxy. disk: A nuclear disk-like structure is seen.